PROGRESS IN APPLIED SCIENCE AND TECHNOLOGY
Faculty of Science and Technology
Rajamangala University of Technology Thanyaburi
Vol.11 No.3 (2021): 9–14
ISSN (Print): 2730-3012
ISSN (Online): 2730-3020
https://ph02.tci-thaijo.org/index.php/past

Received 13th July 2021,
Revised 28th August 2021,
Accepted 18th October 2021

DOI: 10.14456/past.2021.21

Effect of Compatibilizing Agents on Organoclay Dispersion of Polypropylene/Organoclay Nanocomposites

Haydar U. Zaman[1*] and Ruhul A. Khan[1]
[1] *Institute of Radiation and Polymer Technology, Bangladesh Atomic Energy Commission, P.O. Box 3787, Savar, Dhaka, Bangladesh*
*E-mail: haydarzaman07@gmail.com

Abstract

The purpose of this research was to observe the effect of two compatibilizers, namely, maleated polypropylene (denoted as PPM) and potassium succinate-g-polypropylene (denoted as PPK), on the properties of polypropylene (PP)/PPM/organoclay (OC) or PP/PPK/OC ternary nanocomposite. Nanocomposites were made by melt blending PP directly with 5 wt% organoclay (Cloisite 15A, OC) using two separate compatibilizers with a fixed amount of 10 wt%. Transmission electron microscopy (TEM) photographs confirmed that the OC was intercalated and exfoliated within the presence of PP/PPM or PP/PPK during melt mixing. PPK compatibilized systems had better exfoliation of PP/OC nanocomposites than PPM compatibilized systems. Better dispersion and exfoliation state of OC was performed by adding PPK rather than PPM. PP/PPK/OC nanocomposites were found to have the most continuous and uniform size. The PPK compatibilized system has given higher tensile strength and tensile modulus but with less elongation at break (%) than in PPM compatibilized cases. Differential scanning calorimetry (DSC) assessment indicates an increase in melting temperature, crystallization temperature, and crystallinity. Moreover, the addition of PPK or PPM with OC enhances the rheological behaviors of nanocomposites.

Keywords: Polypropylene, organoclay, nanocomposites, compatibilizer, crystallization

1. Introduction

Polymer nanocomposites produced from organoclay attracted increasing interest in situ polymerization as a result of the first synthesis of nylon/clay nanocomposites in the late twentieth century (1). Since organically layered silicate is well dispersed providing high levels of reinforcement at relatively low concentrations, many studies have been conducted primarily on how stacked layered silicates can be dispersed into individual platelets, such as exfoliated or at least intercalated structures. Nanocomposites are highly respected because they often exhibit better mechanical, thermal, and rheological properties than conventional nanocomposites (2, 3). Most nanocomposites promise to be a hybrid with silicate inorganic polymer layers and inorganic clay mineral layers (4, 5). The Toyota investigation team first tested the polyamide-6/clay nanocomposite and found that the mechanical and thermal properties of the clay filler developed at a much lower load stage than conventional composites (6). Polymer/clay nanocomposite has been reported in the scientific literature (7-10). López-Quintanilla et al. (11) report that three types of polymer/clay nanocomposites are generally recognized: ‘‘conventional composites,’’ where clay was added as common filler; “intercalated nanocomposites,” in which a small portion of the polymer was allowed to insert into the interlayer spacing between the layered silicates, and ‘‘exfoliated nanocomposites,’’ in which the layered silicates are well dispersed in a continuous polymer matrix (12, 13).

Polyolefin/layered silicate nanocomposites can be expected to replace metals and high-performance engineering thermoplastics with low cost. Especially, PP is a thermoplastic-engineered non-polar polymer and it is widely used for various uses such as automobiles and packaging due to its versatility, all balanced properties, and attractive property-price ratio. PP/organoclay nanocomposites have been applied for extensive research attention. However, the uniform dispersion of silicate layers in PP cannot be realized due to the low polarity of conventional PP. This is due to the incompatibility between organically modified clay and PP, which have no polar groups in their backbone. Nevertheless, PP/clay nanocomposites have become realistic possibility using compatibilizers such as functional oligomers. This type of compatibilizer must have sufficient polarity to communicate with the silicate layer and easily blending bulk PP (14). To improve the

mineral clay isolation in the PP matrix, investigators typically used maleic anhydride (MA) (15, 16), which can develop the polarity of polymer molecules. Most studies using PP/clay nanocomposite have conducted PP-grafted-MA because it provides the best degree of strengthening effect of all PPs so far. Nguyen et al. (17) showed that use of high concentration of PPK as compatibilizer improved the dispersion of clay in low molecular weight PP. Therefore, in the present study, we tested PPM and PPK as compatibilizers of PP/clay nanocomposite. No literature is available for the best knowledge of the authors on the effects of particular compatibilizers on the morphological, mechanical, thermal, and rheological properties of PP/organoclay nanocomposite by molten mixing technique. Therefore, the effort is to clear this significant information even and emphasize this investigation of mechanical and thermal properties using two different compatibilizers.

2. Experimental

2.1 Materials

The thermoplastic polymer matrix PP was obtained from MTBE (Malaysia) Sdn. Bhd. as the pellets form with a specific gravity of 0.91-0.92 and melting temperature of 160-170°C. Organoclay (trade name: Cloisite 15A) based on dimethyl dehydrogenated tallow quaternary ammonium (2Me2HT) chloride with a cation exchange capacity of 125 meq/100g was supplied by Southern Clay Products, USA. PPMA (melt flow rate: 50 g/10 min at 230°C, 0.5 wt% MA included, grade: Polybond 3150) was obtained from Uniroyal Chemicals.

2.2 Methods

2.2.1 Potassium succinate-grafted polypropylene (PPK) preparation

PPM was diluted with 1,2-dichlorobenzene ($C_6H_4Cl_2$) at 110°C. The indicator (phenolphthalein) was included in a drop solution. The drops were incorporated through a 0.3 N methanolic KOH solution until the paint of the solution was light pink. It was heated for another 30 minutes to confirm the pink paint visibility and full neutrality. PPK was exhausted in MeOH and was refined with hot MeOH; PPK was filtered and dried at 80°C to obtain white paint. PPK was created by instantaneous hydrolysis and mitigation of PPM solution (Scheme 1).

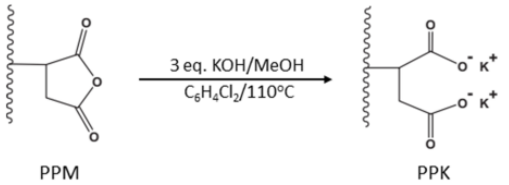

Scheme 1 Preparation of K-g-PP (PPK).

2.2.2 Sample preparations

PP and organically modified clays were slowly dried by weight in a ventilated oven at a temperature of 80°C. The compositions of PP/organoclay nanocomposite are recorded in Table 1.

Table 1 Compositions of PP/organoclay nanocomposite.

Samples	PP wt%	Organoclay wt%	PPM wt%	PPK wt%
PP	100	-	-	-
PPO5	95	5	-	-
PPO5M10	85	5	10	-
PPO5K10	85	5	-	10

PPM: Maleated polypropylene; PPK: potassium succinate-g-polypropylene

The nanocomposites were made using a co-rotating twin-screw extruder ((Brabender Plasticcorder, model: PLE-331) in an organo-clay mixture with PP and compatibilizer. The temperature of the mixture was fixed at 190°C, the screw speed was 50 rpm, and the mixing time of each sample was 8 min. Nanocomposite samples were compressed into sheets of 1 mm thickness at 180°C and 10 MPa for 5 min with compression molding and then cooled to 25°C at the same pressure. Molded sheets were designed to be used for cutting and evaluating various properties.

2.2.3 Morphological studies

2.2.3.1 Transmission electron microscopy (TEM)

Organoclay dispersion in the nanocomposite sample was performed by transmission electron microscope (TEM; JEOL, model JEM-2010, Japan) with an accelerated voltage of 200 kV. The extruded samples were microtomed in the form of ultrathin pieces (approximately 100 nm thickness) by a microtome with a diamond knife (Leica Ultracut UCT) then the pieces were depicted in the TEM.

2.2.3.2 Scanning electron microscopy (SEM)

Extruded samples were fractured with liquid nitrogen and the fracture surface of the sample was observed using Scanning Electron Microscope (SEM; JEOL, model: JSM-6360LV, Japan) at an accelerated voltage of 15 kV. The fracture surfaces of the sample were coated with a thin layer (10–20 nm) of gold before analysis.

2.2.4 Tensile properties

The tensile properties of the composite samples were performed according to ASTM-D 638-14 standard method (18) by a screw-driven universal testing machine (model: Instron 4466, USA). The crosshead speed of 20 mm/min and the gauge length was 10 mm. All samples were conditioned at 25°C and 55% relative humidity.

2.2.5 Thermal properties

2.2.5.1 Differential scanning calorimetry (DSC)

The melting and crystallization temperature and crystallinity of the sample were performed by Differential Scanning Calorimetry (Perkin Elmer,

model: DSC-7, Wellesley, MA, USA) at a heating rate of 10°C/min in the N_2 environment. The weight of the sample was between 5-8 mg

2.2.5.2 Heat distortion temperature (HDT)

HDT of PP and nanocomposites was determined using samples containing 125 × 12.50 × 3.0 mm^3 under the ASTM D 648 method. The test was performed using Advanced HDT/Vicat softening point equipment (Ray Ryan Test Equipment, Ltd, UK) with a heating rate of 2°C/min.

2.2.6 Rheological measurements

The rheological properties (elastic modulus, G′; loss modulus, G′′; and complex viscosity, η*) of the nanocomposite disc samples were measured using the advanced rheometric expansion system (model: ARES Rheometer, USA). To make a disc sample, nanocomposites were compression molded using a hot press at 200°C. All tests were performed in the frequency range of 0.1-100 rad/s at 200°C.

3. Results and Discussion

3.1 TEM analysis

Figure 1 presents TEM photomicrographs of PP/organoclay nanocomposites consisting of PP/5% organoclay (designated as PPO5), PP/10% PPM/5% organoclay (marked as PPO5M10), and PP/10% PPK/5% organoclay (designated as PPO5K10). Figure 1(a) displays considerably bigger organoclay particles, which are not intercalated and probably form a 'micro composite' structure, possibly due to the absence of compatibilizers. The black shape (piled silicate platelets) exhibits the organoclay tactoids and the rest of the region represents an uninterrupted PP. Nevertheless, some black shapes may indicate some weakly dispersed organoclay aggregates. Figure 1(b) on the other hand shows relatively small organoclay particles compared to Figure 1(a) and the organic particles were separated into lighter parts by the blending manner. From the TEM micrographs, it is clear that nanocomposites made with 10 wt% PPK as compatibilizer show mostly exfoliated structures where organoclay layers are completely delamination and dispersed evenly in the polymer matrix Figure 1(c) while the nanocomposites made with 10 wt% PPM as compatibilizer showed clusters of organoclay layers suggesting intercalated structures Figure 1(b). In general, organoclay dispersion in a high molecular weight PP is considered difficult using a compatibilizer similar to PPM. However, an ionomer such as PPK was found to be an efficient compatibilizer even for a high molecular weight PP resulting in the formation of well-dispersed nanocomposites. Therefore, compatibilizers should be mixed with organoclay and PP to better disperse organoclay in the matrix and enhance the mechanical properties.

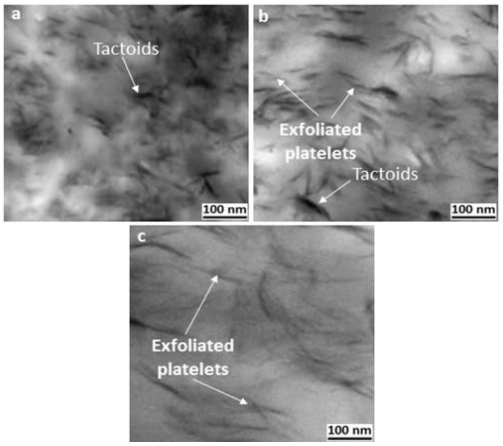

Figure 1 TEM images for three nanocomposites: (a) PPO5, (b) PPO5M10, and (c) PPO5K10.

3.2 Scanning electron microscopy analysis

SEM photomicrographs of PPO5, PPO5M10, and PPO5K10 nanocomposites are displayed in Figure 2. The organoclay particles in Figure 2(a) were randomly distributed in the PP matrix and some large portions were visible above the fracture surface. Large particles are dispersed in PP to PPO5 nanocomposite so that no functional polymer is present and the interfaces appear to be individually wet and/or weak to the adhesion of the particles. Figures 2(b) and (c) display photomicrographs of PPO5M10 and PPO5K10 nanocomposites. The PPO5M10 system had some large parts and the average particle size was smaller than the PPO5 system. As shown in Figure 2(c), the PPO5K10 system was more uniformly dispersed in the PP matrix than the PPO5M10 system. Changes in both particle size and interface indicate that PPO5M10 or PPO5K10 helps to break down particles and modify interfacial interactions. This result agrees with the outcomes of the mechanical properties in Table 2.

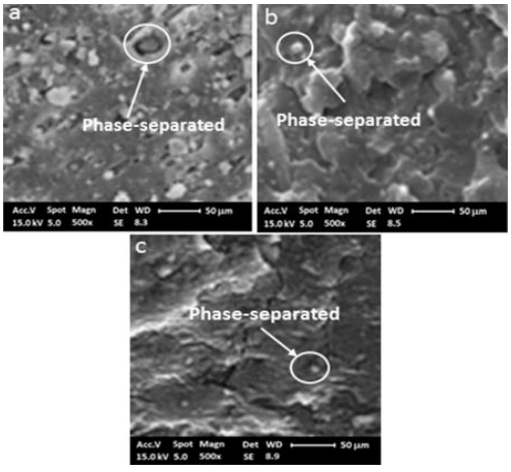

Figure 2 SEM photomicrographs of (a) PPO5, (b) PPO5M10, and (c) PPO5K10 nanocomposites.

3.3 Tensile properties evaluation

In general, the tensile properties (tensile strength, TS; tensile modulus, TM; and elongation at break, Eb (%)) of immiscible mixtures without compatibility are weak due to weak interfacial bonding between the components. Tensile properties were measured in neat PP and PP/organoclay nanocomposites with a certain amount of 5 wt% loaded with organoclay and 10 wt% in the presence of compatibilizers. It was important to note how both compatibilizers performed in tensile properties. The test results of the tensile properties are recorded in Table 2. The tensile properties of neat PP were significantly improved by incorporating organoclay and PPM or PPK. The TS and TM of neat PP were approximately 29.7 and 1133 MPa, and the corresponding values for nanocomposite were raised to 35.5 and 1315 MPa, respectively. Increased tensile properties may improve the interfacial bonding between the matrix and organoclays due to the long aliphatic chains in cloisite 15A. Also, the TS and TM of the nanocomposite associated with PPO5K10 had the highest values in all cases tested on specific organoclay content. The highest values achieved were 41.2 and 1603 MPa, an increase of 39 and 42% over virgin PP, respectively. In contrast, there was a somewhat increase in the TS of the nanocomposite of PPO5M10. The increased tensile properties of a compatibilized system (compared to an unmodified system) are usually explained by the fine dispersion and increased solid-state adherence produced by the compatibilizer, which can transfer more stress from the matrix to the dispersion phase. These results are consistent with the results of research studies conducted by W.C. Chen et al. (19). The elongation at break is a significant tensile property for materials. Generally, the inclusion of organoclay in polymeric substances reduces the elongation at break. Follow this trend of elongation at break of nanocomposite as shown in Table 2, the same organoclay and PPM or PPK content.

Table 2 Compositions and tensile properties of PP/organoclay nanocomposites.

Samples	PP wt%	OC wt%	PPM wt%	PPK wt%	TS (MPa)	TM (MPa)	Eb (%)
PP	100	-	-	-	29.7±0.7	1137±43	9 ±1.2
PPO5	95	5	-	-	35.5±0.6	1315±59	85±1.3
PPO5M10	85	5	10	-	37.9±0.5	1185±52	74±1.5
PPO5K10	85	5	-	10	41.2±0.9	1603±60	71±1.4

OC: Organoclay; PPM: maleated polypropylene; PPK: Potassium succinate-g-PP; TS; tensile strength; TM: tensile modulus; Eb: elongation at break

3.4 DSC measurements

The results of crystalline and melting peak temperatures of neat PP and its nanocomposites are illustrated in Figures 3(a) and 3(b), respectively. Figure 3(a) displays that the crystallization peak temperature (T_c) improved from 112.2°C of PP to 114.2°C of PPO5 nanocomposite. It is noteworthy that the T_c of PPO5K10 has been elevated to 117.8°C, which is much larger than PP and larger than PPO5M10 nanocomposite. In this way the PP crystallization process has an exaggerated effect on the compatibilizer and organoclay, which is probably due to the increase in the PP melt viscosity of the organoclay, increasing the local shear stress, and the compatibilizer in PPO5K10 forms a more homogeneous network structure. Furthermore, the T_m of PP was affected by the inclusion of organoclay and/or compatibilizers due to the induced perfect crystalline [Figure 3(b)]. The degree of crystallinity (%) of neat PP and its nanocomposites are displayed in Figure 4(a). Organoclay has an imperfect effect on crystallinity since the compatibilizer makes great enhancement of crystallinity in both PPO5M10 and PPO5K10 systems. To consider the nucleation effect of the compatibilizer in PP, one can assume that the crystallinity of PP in PPO5K10 is mostly determined by the compatibilizer rather than the organoclay. Since the above results were very naturally attractive, organoclay was considered an effective nucleating agent due to its superior surface area at the time of exfoliation. However, due to the effects of welding, plasticizing, and/or the defects mentioned, the nucleation efficiency of the interface decreases. In particular, the high nucleating efficiency of organoclay was hampered by the high proportion of compatibilizers (20).

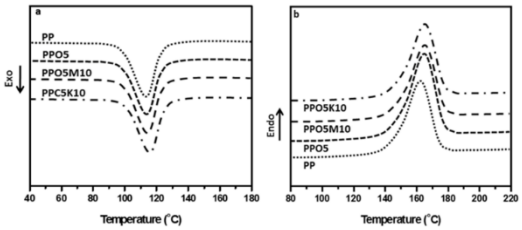

Figure 3 Differential scanning calorimetry (DSC) (a) crystallization and (b) melting curves of polypropylene (PP) and its nanocomposites.

3.5 Heat distortion temperature (HDT)

Figure 4 (b) demonstrates the thermal behavior of PP and its nanocomposites as measured in HDT. The HDT of PPO5 systems was about 2.1°C higher than that of neat PP; this is mainly due to the well-dispersed organoclay platelets within the matrix as will be seen in the TEM results. This confirms the improved thermal stability of the PPO5 system with the presence of organoclay particles. The improvement in HDT could be attributed to the presence of strong hydrogen bonds between the polymer matrix and clay surface (21). Another reason for this was the improved mechanical stability of nanocomposites and the increase in melting temperature, which varied in nanocomposites compared to neat PP. Compared with the PPO5 system, due to better dispersion and exfoliation of organoclay layers in the polymer matrix, the PPO5M10 system has shown a more progressive

improvement in HDT. Furthermore, the PPO5K10 system showed the highest value in HDT among all samples. This may be attributed to the better-exfoliated structure in the PPO5K10 nanocomposite as confirmed by TEM results discussed earlier. In other words, compatibilizers have a synergistic effect in improving the thermal properties of PP.

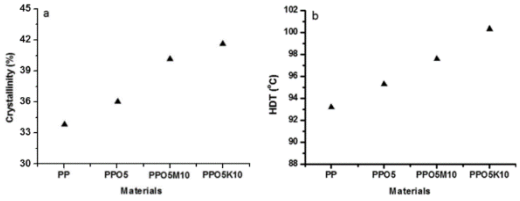

Figure 4 (a) Crystallinity of PP, PPO5, PPO5M10, and PPO5K10; and (b) Hardness properties of PP, PPO5, PPO5M10, and PPO5K10 nanocomposites.

3.6 Viscoelastic behavior

The study of melt rheology is very significant from a polymer-processing perspective. In addition, it gives the idea of a microstructure in a molten state. Figure 5(a)-(c) provides the storage modulus (G′), loss modulus (G″), and complex viscosity (η*) of the neat PP, PPO5, PPO5M10, and PPO5K10 systems as a function of the frequency, respectively. Significant effects of nanocomposites show organoclay compared to linear viscoelastic responses. The G′, G″, and η* of the PP matrix were increased by employing organoclay. It has been observed that PPO5K10 has the maximum range of the frequencies studied in G′ and G″ (Figures 5a and 5b). Particularly in the low-frequency region, it has been observed that the G′ and G″ frequencies become distinct for PPO5K10 and PPO5M10 that are characteristic behaviors of hard-core materials. Increases of G′ and G″ at lower frequencies indicate a stronger interaction between the organoclay layer and the polymer matrix. The outcomes indirectly display no interaction between the organoclay layer and the PP chain, and PPO5 could not demonstrate substantial filler influence deprived of a compatibilizer. On the contrary, to consider the increase in G′ and G″ terminal regions, it has been demonstrated that PPO5M10 produces a considerable interaction at the interface between the polymer and organoclay layers, yet it is less than the sample sorted with PPO5K10 at a specific organoclay content. Expect organoclay layers to display better dispersion in the PPO5K10 system than in the PPO5M10 system for the given sample composition.

Figure 5(c) displays the complex viscosity (η*) versus frequency for PP, PPO5, PPO5M10, and PPO5K10 systems achieved from the frequency sweep exam. The nanocomposite decreases with increasing frequency of η* and indicates "non-Newtonian behavior". The observed behavior of shear-thinning nanocomposites can be attributed to the orientation of strong molecular chain adaptation of polymer nanocomposite during applied shear forces. The influence of compatibilizers on the η* of the nanocomposites was more frequent at lower frequencies than at higher frequencies, and with the addition of compatibilizers, this influence decreases with increasing frequency due to the strong shear-thin behavior of polymer nanocomposites. It was observed that PPO5K10 produced a substantial interaction at the interface between the polymer and the clay layer, which was improved than the prepared sample with PPO5M10 at a certain organoclay content. This enrichment influence was intimately related to the large growth in the G′ or G″.

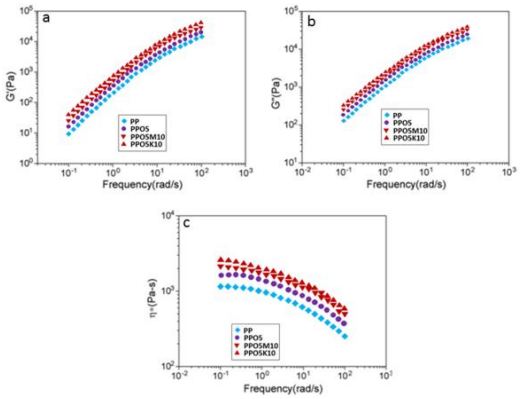

Figure 5 Neat PP, PPO5, PPO5M10, and PPO5K10 nanocomposites of (a) G′, (b) G″, and (c) η* as a function of the frequency.

4. Conclusions

In this research, PP/organoclay nanocomposites were successfully prepared using maleated polypropylene (PPM) and potassium succinate-grafted-polypropylene (PPK) as compatibilizers. Both compatibilizers were effective in assisting the silicate platelet delamination. PPM was beneficial in achieving the partial exfoliation of the PP/organoclay nanocomposites in comparison with PPK. SEM images showed that adding a compatibilizer could decrease the size of phase-separated particles, which made the material more uniform. The addition of compatibilizer into PP/organoclay has been proven to not only enhance the degrees of intercalation but also at the same time improves the mechanical properties. The PPK compatibilized system conferred higher tensile properties than the PPM compatibilized system and the PP/organoclay case. This indicates that the PPM compatibilizer has lower polarity than PPK, and promotes less effective interaction between organoclay and polymer matrix. DSC thermograms showed that added compatibilizers with increased crystallization and melting temperatures and crystallinity of nanocomposite. Rheological analysis suggested an increase in the storage modulus, loss modulus, and complex viscosity of the nanocomposites compared to the polymer matrix.

Declaration of conflicting interests

The authors declared that they have no conflicts of interest in the research, authorship, and this article's publication.

References

1. Ray S.S., Okamoto M. Polymer/layered silicate nanocomposites: a review from preparation to processing. Prog Polym Sci. 2003; 28: 1539-641.
2. Pesetskii S., Bogdanovich S., Aderikha V. Polymer/clay nanocomposites produced by dispersing layered silicates in thermoplastic melts. Research Anthology on Synthesis, Characterization, and Applications of Nanomaterials: IGI Global. 2021; 1002-30.
3. Zaman H.U., Hun P.D., Khan R.A., Yoon K.-B. Comparison of effect of surface-modified micro-/nano-mineral fillers filling in the polypropylene matrix. J Thermoplast Compos. 2013; 26: 1100-13.
4. Mukhopadhyay R., Bhaduri D., Sarkar B., Rusmin R., Hou D., Khanam R., et al. Clay–polymer nanocomposites: Progress and challenges for use in sustainable water treatment. J Hazard Mater. 2020; 383: 121125.
5. Monjarás-Ávila A.J., Sanchez-Olivares G., Calderas F., Moreno L., Zamarripa-Calderón J.-E., Cuevas-Suárez C.E., et al. Sodium montmorillonite concentration effect on Bis-GMA/TEGDMA resin to prepare clay polymer nanocomposites for dental applications. Appl Clay Sci. 2020; 196: 105755.
6. Hammami I., Hammami H., Soulestin J., Arous M.Kallel A. Thermal and dielectric behavior of polyamide-6/clay nanocomposites. Mater Chem Phys. 2019; 232: 99-108.
7. Tan H., Wang L., Wen X., Deng L., Mijowska E., Tang T. Insight into the influence of polymer topological structure on the exfoliation of clay in polystyrene matrix via annealing process. Appl Clay Sci. 2020; 194: 105708.
8. Kodali D., Uddin M.-J., Moura E.A., Rangari V.K. Mechanical and thermal properties of modified Georgian and Brazilian clay infused biobased epoxy nanocomposites. Mater Chem Phys. 2020; 257: 1-13.
9. Rigail-Cedeño A., Schmidt D.F., Vera G., Chavez M., Pacheco Y., Alava M., editors. Elastomeric bio-based epoxy/clay nanocomposites. AIP Conf Proc. 2020; AIP Publishing LLC.
10. Irandoost M., Pezeshki-Modaress M., Javanbakht V. Removal of lead from aqueous solution with nanofibrous nanocomposite of polycaprolactone adsorbent modified by nanoclay and nanozeolite. J Water Proc Eng. 2019; 32: 100981.
11. López-Quintanilla M., Sánchez-Valdés S., Ramos de Valle L., Medellín-Rodríguez F. Effect of some compatibilizing agents on clay dispersion of polypropylene-clay nanocomposites. J Appl Polym Sci. 2006; 100: 4748-56.
12. Jeon H.G., Jung H.-T., S. Lee W., Hudson S.D. Morphology of polymer/silicate nanocomposites. High density polyethylene and a nitrile copolymer. Polym Bull. 1998; 41:107-13.
13. Effects of process conditions and mixing protocols on structure of extruded polypropylene nanocomposites. J Appl Polym Sci. 2004; 93(4):1891-99.
14. Casalini T., Rossi F., Santoro M., Perale G. Structural characterization of poly-l-lactic acid (PLLA) and poly (glycolic acid)(PGA) oligomers. Int J Mol Sci. 2011; 12: 3857-70.
15. Bunekar N., Tsai T.-Y., Huang J.-Y., Chen S.-J. Investigation of thermal, mechanical and gas barrier properties of polypropylene-modified clay nanocomposites by micro-compounding process. J Taiwan Inst Chem E. 2018; 88: 252-60.
16. Wu M.-H., Wang C.-C., Chen C.-Y. Preparation of high melt strength polypropylene by addition of an ionically modified polypropylene. Polymer. 2020; 202: 122743.
17. Nguyen V.K., Jin S.H., Lee S.H., Lee D.S., Choe S. Polypropylene/clay nanocomposites prepared with masterbatches of polypropylene ionomer and organoclay. Compos Interface. 2006; 13: 299-310.
18. American Society for Testing and Materials. D638−14 Standard Test Method for Tensile Properties of Plastics. Standard Test Method for Tensile Properties of Plastics. 2014; 17.
19. Chen W.C., Lai S.M., Chen C.M. Preparation and properties of styrene–ethylene–butylene–styrene block copolymer/clay nanocomposites: I. Effect of clay content and compatibilizer types. Polym Int. 2008; 57: 515-22.
20. Zhong W., Qiao X., Sun K., Zhang G., Chen X. Polypropylene–clay blends compatibilized with MAH-g-POE. J Appl Polym Sci. 2006; 99: 2558-64.
21. Shaobo X., Shimin Z., Fosong W., Huiju L., Mingshu Y. Influence of annealing treatment on the heat distortion temperature of nylon-6/montmorillonite nanocomposites. Polym Eng Sci. 2005; 45(9): 1247-53.